Protoenzymes: The Case of Hyperbranched Polymer-Scaffolded ZnS Nanocrystals

Irena Mamajanov,[1,*] Melina Caudan,[1] Tony Z. Jia[1,2]

[1] Earth Life Science Institute, Tokyo Institute of Technology, Meguro, Tokyo 152-8550, Japan.
[2] Blue Marble Institute for Science, 1001 4th Ave, Suite 3201, Seattle, WA 98154, USA.
* Correspondence: irena.mamajanov@elsi.jp

Abstract: Enzymes could be described as small-molecule, metal, or cluster catalysts augmented by biopolymeric scaffolds. It is conceivable that early in chemical evolution, ancestral enzymes opted for simpler, easier to assemble scaffolds. Herein, we describe such possible protoenzymes: hyperbranched polymer-scaffolded metal-sulfide nanocrystals. Hyperbranched polyethyleneimine (HyPEI) and glycerol citrate polymer-supported ZnS nanocrystals (NCs) are formed in a simple, abiotically plausible process. Transmission electron microscopy (TEM) analyses of HyPEI-supported NCs reveal spherical particles with an average size of 10nm that undergo only a modest aggregation over a 14-day incubation. The polymer-supported ZnS NCs are shown to possess a high photocatalytic activity in an eosin B photodegradation assay, making them an attractive model for the study of the origin of life under the "Zn world" theory dominated by a photocatalytic proto-metabolic redox reaction network. The catalyst, however, could be easily adapted to apply broadly to different protoenzymatic systems.

Keywords: protoenzyme; hyperbranched polymers; photocatalytic nanoparticles; polymer-supported nanoparticles; metal-sulfide clusters

1. Introduction

Metabolism is one of the defining characteristics of life. The primary purpose of metabolism is the efficient utilization of external sources of energy to fuel cellular processes, such as growth and replication [1]. Enzymes, highly selective and efficient biocatalysts, govern metabolism. Enzymes offer a selective advantage to some reactions by enhancing their rate up-to 10^{23}-fold [2,3], unmatched by other types of catalysts, effectively shaping metabolic transformations. This level of control and order sets metabolism apart from any other set of chemical reactions. The crucial role of enzymes in life has prompted some to argue that catalytic enzyme precursors, or protoenzymes, played a critical role in the emergence of life [4,5].

Nearly all enzymes are based upon globular proteins, save for some RNA strands that have catalytic activity (ribozymes) [1]. While the discovery of the ribozyme [6,7] has become the basis of the RNA world origins of life theory [8,9], the question of how long, functional biopolymers were spontaneously formed remains unsolved. Previous studies have thus considered potentially more prebiotically reasonable transition metal complexes [10], small molecules [11], and mineral surfaces [12, 13] as primitive protoenzymes. While metal cations and small molecules catalyze chemical reactions by lowering the activation energy or altering reaction pathways, macromolecular enzymes offer an additional advantage of selective binding, orienting, and enclosing reactants within a modulated microenvironment [14]. In the prebiotic world, in the absence of long coded proteins or RNA, mineral surface catalysis could have performed some catalytic functions. Encapsulation of organic molecules between mica sheets has been proposed to trigger protoenzymatic processes [15] and clay minerals have been shown to facilitate the polymerization of activated nucleotides, presumably by orienting the reactants [16]. The orientation of glycine molecules on oxide mineral surfaces has also been shown to affect its reactivity towards polymerization [17].

In the synthetic community, the application of enzymatic systems to modern synthetic processes has become a desirable goal [18]. The high cost of enzyme isolation and enzyme incompatibility with synthesis conditions outside of physiological has prompted studies of non-biopolymer-based enzyme mimics. Approaches to the design of artificial enzymes range from stripping the cofactors of the biopolymeric scaffold, synthesis of supramolecular active sites, surveying enzyme-mimetic properties of various nanoparticles, and investigation of non-biological polymeric scaffolds [19]. In the context of prebiotic chemistry, it is conceivable that the first enzymes may not have been purely or entirely protein- or RNA-based. Herein, we describe an effort to combine the principles of artificial enzyme construction discovered by synthetic chemists to gain new insights into the question of the provenance of enzymes.

Catalytic nanoparticles are an attractive avenue to explore in the context of protoenzymes. The catalytic properties of nanoparticles, in particular, arise from their large surface area compared to the nanoparticle's total number of atoms [20]. Many nanoparticle catalysts have been shown to catalyze enzymatic reactions to earn the term "nanozyme" [21]. Nanomaterials are usually thought of as synthetic or anthropogenic; however, they can form through natural abiotic processes and could have been present on prebiotic Earth. All mineral formation processes undergo a sometimes persistent nanophase stage during formation. For example, volcanic ash clouds contain polydisperse particles that range from 100 to 200 nm in size and are primarily composed of silicate and iron compounds [22]. In geological processes, nanoparticles can be generated through mineral weathering or by mechanical grinding associated with earthquake-generating faults in Earth's crust [23]. Could chemical evolution harness the catalytic capacity of natural nanomaterials? To answer this question, we investigated the potential role of metal-sulfide nanocrystals (NCs) as possible precursors to metal sulfide clusters found in some modern enzymes. Metal sulfide deposits near deep-sea hydrothermal vents have become the basis of the iron-sulfur world theory [24]. The model suggests that these minerals would catalyze complex sequences of reactions, driven by the energy from the vents, eventually leading to life. In the subaerial "Zinc world" scenario [25], life emergence would have been driven by light energy harnessed by photoactive semiconductive zinc sulfide (ZnS) minerals. Under "Zinc world" assumptions, the geochemical formation of long-lived ZnS nanoparticles would extend the catalytic capacity of the material due to the significantly increased specific surface area of the catalyst and the exciton confinement effects [26]. NCs, however, tend to spontaneously aggregate; therefore, it is a common practice to include polymeric supports [27] or other capping agents [28,29] in NC formulations to decrease particle overgrowth and aggregation. As a plausible prebiotic polymeric support candidate, we introduce hyperbranched polymers. Hyperbranched polymers [30] and dendrimers [31,32] have been long considered for biomimetic catalysts in synthetic applications. Our previous studies have demonstrated the plausibly prebiotic synthesis of hyperbranched polyesters from citric acid and glycerol [33-35] and the ability of hyperbranched polyesters to catalyze the Kemp elimination reaction [36]. Here, we report on the prebiotically plausible formation of photocatalytic hyperbranched polymer-scaffolded ZnS NCs.

2. Materials and Methods

All chemicals were purchased from Sigma-Aldrich (St. Louis, MO, USA) and used without further purification.

Synthesis of hyperbranched polyethyleneimine (HyPEI)-supported ZnS nanocrystals (NCs):

To produce 10mg of supported ZnS NCs, a solution of 0.4g HyPEI (124.9ml, pH=6) was titrated with 2.56ml of 40mM $ZnCl_2$ solution and magnetically stirred for 1 hour. 2.56mL of a 40mmol solution of Na_2S was then added dropwise and was allowed to stir for 1 hr magnetically.

Synthesis of glycerol citrate polyesters:

A polyesterification was conducted, starting with 10mL of an aqueous solution containing 330mM citric acid and 660mM glycerol. Some formulations contained also 165mM $CoCl_2$ or $ZnCl_2$. The samples were incubated, uncovered, at 85°C for 72 h. The resulting gel-like product was redissolved and dialyzed through a 500-1000Da cutoff Float-A-Lyzer membrane (Repligen, Waltham, MA, USA) and lyophilized.

Measurement of the divalent cation loading capacity of the polymers: 100mg of glycerol citrate polyester (formulation without added cations), COOH-terminated oligo- 2,2-bis(hydroxymethyl)propionic acid dendrimer, trimethylol propane core, generation 1, $C_{45}H_{62}O_{30}$ (Sigma-Aldrich, 806099), OH-terminated oligo- 2,2-bis(hydroxymethyl)propionic acid dendrimer, trimethylol propane core, generation 1, $C_{21}H_{38}O_{12}$(Sigma-Aldrich, 805920) polyester dendrimers, and HyPEI was equilibrated overnight in 1mL of a 165mM solution of $CoCl_2$. The step was omitted for the glycerol citrate polyesters prepared in the presence of $CoCl_2$. The solutions were then dialyzed through a 500-1000Da cutoff Float-A-Lyzer membrane and lyophilized. The content of Co^{2+} per unit weight of the resulting polymer was determined spectroscopically utilizing a JASCO (Hachioji, Tokyo, Japan) V-670 UV-vis spectrometer.

Synthesis of glycerol citrate polyester-supported ZnS NCs: The loading capacity towards the absorption of Zn^{2+} was estimated to be the same or similar, as in the case of Co^{2+} ions. An excess of the theoretical amount of the Zn^{2+}-bearing polyester was used. 0.8g of Zn^{2+} -bearing polyester was dissolved in 27.4mL of water. The pH of the solution was adjusted to pH=6 with NaOH. 2.56mL of a 40mmol solution of Na_2S was then added dropwise and was allowed to stir for 1 hr magnetically.

Mass spectrometry: MALDI-MS spectra were collected on an ultrafleXtreme Bruker Daltonics MALDI-TOF-MS (Bruker Corporation, Billerica, MA, USA) in positive ion mode. External mass calibration was conducted using standard peptide mixtures. The sample preparation matrix, 90:10 mixture of 2,5-dihydroxybenzoic acid and 2-hydroxy-5-methoxy benzoic acid (SDHB), was dissolved in deionized water. Subsequently, the freeze-dried samples and the matrix were mixed at a 1:10 [v/v] ratio in advance, and then the mixture was applied to the plate before analysis.

Transmission Electron Microscopy (TEM): Transmission Electron Microscopy and Field-emission (FE)-TEM imaging were performed at the Tokyo Institute of Technology Materials Analysis Division Technical Department in Meguro-ku, Tokyo, with the assistance of Akira Genseki and Ryohei Kikuchi. Samples were prepared by placing a droplet of ZnS nanoparticle solution (See above for synthesis method) on a Collodion Film COL-C15 copper grid (Okenshoji Co., Ltd., Chuo-ku, Tokyo, Japan) and wicking away the liquid to deposit a thin layer onto the grid. The grid was allowed to dry at room temperature for 2 days before imaging. After confirmation using a Hitachi (Chiyoda-ku, Tokyo, Japan) H7650 Zero A TEM (100 kV), high-resolution imaging was performed at room temperature on a JEOL (Akishima, Tokyo, Japan) JEM-2010F FE-TEM at 200 kV with the following specifications: a ZrO/W(100) Schottky cathode, ultra-resolution pole piece, Gatan (Sarasota, Florida, USA) Digiscan System Model 688, Gatan MSC 794 CCD Camera, and an EDAX (Minato-ku, Tokyo, Japan) Genesis energy dispersive X-ray spectrometer.

Photocatalytic activity measurement: A jacketed pyrex flask (capacity ca. 40mL) was used as the photoreactor vessel. For a typical experiment, a solution adjusted to pH=6 by NaOH containing eosin B (5.0 x10-5M, 30mL) and polymer-supported ZnS NC catalysts (10mg of ZnS, corresponding amount of polymer) was magnetically stirred in the dark for 30 min to reach the adsorption equilibrium of eosin B with the catalyst and then exposed to light from a 100W high-pressure mercury lamp (Handy 100, Mizuka Planning, Amagasaki, Hyogo, Japan). The temperature of the solution was maintained constantly by circulating ice water through the flask's jacket. An aliquot was collected every 15 min; UV/Vis absorption spectra of each aliquot were recorded on a JASCO V-670 UV-vis spectrometer.

3. Results

The procedure for the preparation of hyperbranched polyethyleneimine (HyPEI) was adapted from a protocol described by Hassan and Ali [37]. The protocol devised by Hassan and Ali utilized high molecular weight HyPEI (M_w=25,000 – 50,000); however, we used HyPEI of a low molecular weight HyPEI (M_w=800Da) comparable to that of hyperbranched polyesters synthesized under prebiotically plausible conditions [33,34] In our experiments, when Na_2S solution was titrated into a solution of $ZnCl_2$ at neutral pH, the clear solution quickly turned cloudy with a white precipitate, presumably, crystalline zinc sulfide (ZnS), settling within an hour. However, when Na_2S solution was titrated into a $ZnCl_2$ solution in the presence of hyperbranched polyethyleneimine (at neutral pH, the resulting solution remained unclouded for at least 14 days suggesting that the ZnS product remained

soluble. Figure 1A shows a low-magnification TEM (transmission emission microscope) micrograph of a freshly prepared ZnS/HyPEI sample, which indicates that the sample contains many nanoparticles in a clustered pattern, possibly owing to the hyperbranched polymer matrix. The high-magnification FE (field-emission)-TEM micrograph in Figure 1A (inset) reveals spherical particles with an average size under 10nm. The low-magnification TEM micrograph in Figure 1B shows the presence of aggregated particles (~50nm in diameter) in a solution of ZnS/HyPEI that was kept at room temperature for 14 days, confirming our previous observation that the nanoparticular ZnS remained stable in solution for this time period.

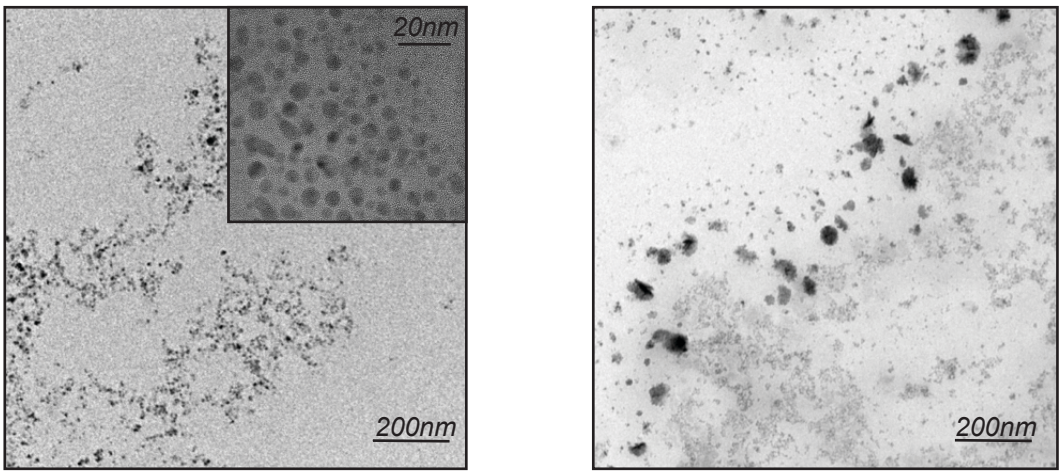

Figure 1. TEM images of HyPEI-supported ZnS nanocrystals. **(a)** Low magnification image of a freshly prepared sample; inset: high magnification FE-TEM micrograph of a freshly prepared sample. **(b)** Low magnification image of a sample aged for 14 days.

HyPEI contains abundant primary, secondary, and tertiary amine groups, and has a strong affinity towards the complexation of transition metals [38]. HyPEI, consequently, has been used in water treatment and as a support for nanoparticles [37,39], although it is not very prebiotically plausible. We, therefore, next considered hyperbranched polyesters that could plausibly form in geochemical settings [33-35]. We assessed the hyperbranched polyesters formed upon the reaction between citric acid and glycerol, as well as commercially available oligo-2,2-bis(hydroxymethyl)propionic acid dendrimers terminated with either carboxylic acid or alcohol functional groups. Neither commercial polyester dendrimers nor the glycerol citrate polymer has exhibited high affinity towards transition metal binding (Table 1). Interestingly, the citric acid glycerol polymers formed in the presence of $CoCl_2$ retained a significant amount of Co^{2+} through dialysis (see the Materials and Methods section). We have previously shown that the presence of divalent cations during citric acid and glycerol polyesterification alters the structure and the size of the resulting polymer [33]. The cation-containing formulations resulted in shorter polymers that incorporated more citric acid moieties compared to neat solution formulations. Stochiometrically, the increased number of citric acid moieties, in turn, increases the number of unreacted carboxylic groups changing the metal affinity. The response of the polyesterification system to the presence of divalent cations by adjusting the polymer product structure to accommodate cation absorption is an example of rudimentary molecular imprinting, a primitive mechanism of molecular memory encoding suggested to be prevalent in prebiotic word prior to the onset of nucleic acid replication [40]. Thus, to incorporate a prebiotically plausible polymer that has molecular imprinting ability, we synthesized a polyester by heating at 85°C a dry mixture of citric acid, glycerol, and $ZnCl_2$ (1:2:0.5, mole ratios). The mass spectral analysis of the polymer (Figure S1) reveals a heterogeneous mixture of polymeric products up to ~1400Da. The resulting polymer solution was titrated with Na_2S to form polymer-scaffolded ZnS NCs.

Table 1. Loading Capacity of Co^{2+} of hyperbranched polyesters and HyPEI.

Polymer	Co^{2+} Loading Capacity ([μmol Co^{2+}/ g polymer]
Hyperbranched Polyethyleneimine Mw=800	736
COOH-terminated oligo- 2,2-bis(hydroxymethyl)propionic acid dendrimer, trimethylol propane core, generation 1, $C_{45}H_{62}O_{30}$ (bis-MPA-COOH)	4.5
OH-terminated oligo- 2,2-bis(hydroxymethyl)propionic acid dendrimer, trimethylol propane core, generation 1, $C_{21}H_{38}O_{12}$ (bis-MPA-OH)	1.6
Citric acid – glycerol polymer, prepared in neat	non detectable
Citric acid – glycerol, prepared in the presence of $CoCl_2$	542

To demonstrate the potential applicability of the polymer-supported ZnS NCs to the prebiotic chemistry in "Zinc world" settings, we have followed the analytical procedure described by Hu et al. [41]. We investigated the photocatalytic activity of the polymer-supported ZnS NCs relative to those of bulk ZnS and the commercial photocatalyst TiO_2 (21nm), with the photocatalytic degradation of eosin B as a test reaction. We have chosen the characteristic absorption of eosin B at 520 nm as the monitored parameter for the photocatalytic degradation process. 30 ml of $5.0x10^{-5}$M solution of eosin B was subjected to incubation with periodic sampling under the following conditions (Figures 2, S2): a) without a catalyst, in the dark b) without a catalyst, under UV irradiation, c) with polyester-supported ZnS NCs (10mg of NCs), in the dark, d) with HyPEI supported ZnS NCs, in the dark, e) with 21nm TiO_2 nanoparticles, in the dark f) with 21nm TiO_2 nanoparticles, under UV, g) with HyPEI-supported ZnS NCs, aged at room temperature for 14 days, under UV h) with freshly prepared HyPEI-supported ZnS NCs, under UV, i) with polyester-supported ZnS NCs, under UV, j) with unsupported ZnS_2, k) with monomeric citric acid, glycerol, $ZnCl_2$, and Na_2S, under UV. When appropriate, 10 mg of TiO_2 nanoparticles or ZnS NCs was used. Under the experimental conditions from (a) to (e), the photocatalytic effect on the solution degradation without catalysts but under exposure to UV light is almost the same as that with catalyst but no exposure to UV light. For example, a slight decrease in the concentration of eosin B was detected in the absence of any catalyst (Figure 2, curve b). Exposure to UV light for 135 min resulted in only 5-6% degradation of the dye with and without the catalyst. The curves measured under the experimental conditions (f) to (i), those containing a catalyst and with exposure to UV light, are indicative of a significantly higher catalytic activity. For example, the fresh HyPEI-supported ZnS NC (Figure 2, curve h) sample was completely decolorized after 135 min of exposure to UV light with a half-life of ~24 mins. The aged HyPEI-supported ZnS NC (Figure 2, curve g), and commercial TiO_2 particle (Figure 2, curve f) samples exhibit a lower photocatalytic activity with half-lives of ~45 and 72 min, respectively. This difference in the photocatalytic activity between fresh HyPEI-ZnS NC sample and aged HyPEI ZnS NC and TiO_2 samples can be explained by the smaller diameter of the ZnS NC (~10nm of the fresh HyPEI-ZnS NCs vs. 20nm of TiO_2 particles vs. ~50nm of the aged HyPEI-ZnS NCs), hence resulting in a larger catalytic surface area. The polyester-supported ZnS NCs activity (Figure 2, curve i) closely resembles that of the fresh HyPEI-supported ZnS NCs (Figure 2, curve h). Unsupported ZnS undergoes quick aggregation and precipitation under the irradiation (Figures S2, S3). In this sample (Figure S2, curve

j), the solution was rapidly decolorized. However, the dye was adsorbed and preserved on the surface of the precipitated ZnS particles suggesting that decolorization derived from the solid-liquid phase partitioning rather than photodegradation (Figure S3). The photocatalytic activity of polyester-supported ZnS NCs was further compared to that of a solution containing *unreacted* citric acid and glycerol as well as $ZnCl_2$ and Na_2S (Figure S2, curve k). Interestingly, ZnS did precipitate out of the solution containing citric acid and glycerol as it did in a neat solution. Moreover, citric acid, glycerol, $ZnCl_2$, and Na_2S solution did not exhibit a detectable photocatalytic activity. It is conceivable that the process of chelation of zinc cations by the unreacted citric acid in the sample (i) interferes with the formation of ZnS particulates.

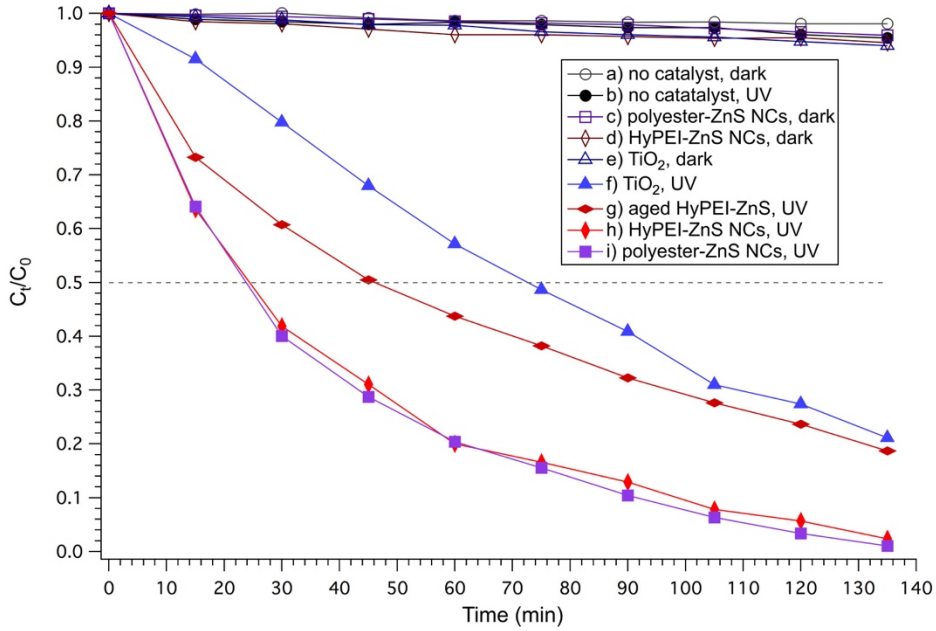

Figure 2. Time-lapse measurement of photodegradation of eosin B ($5.0x10^{-5}$M, 30mL) under different conditions: a) without a catalyst, in the dark b) without a catalyst, under UV irradiation, c) with polyester-supported ZnS NCs (10mg of NCs), in the dark, d) with HyPEI-supported ZnS NCs, in the dark, e) with 21nm TiO_2 nanoparticles, in the dark f) with 21nm TiO_2 nanoparticles, under UV, g) with HyPEI-supported ZnS NCs, aged at room temperature for 14 days, under UV h) with freshly prepared HyPEI-supported ZnS NCs, under UV, i) with polyester-supported ZnS NCs, under UV. When appropriate, 10 mg of TiO_2 nanoparticles or ZnS NCs was used. The normalized concentration (C_t/C_0) was derived from the UV absorbance values at 520nm.

4. Discussion

Our results show that HyPEI- or glycerol citrate polyester-supported ZnS NCs make excellent photocatalysts. Their straightforward formation makes them plausible agents at the early stages of chemical evolution. While we so far have only explored the catalyst and the processes relevant to the "Zinc World" scenario, the demonstrated synthesis of the catalytic complexes could be applicable in a variety of geological settings. Therefore, by considering different particles or cofactors, as well as different plausible polymeric scaffolds, one could extend the repertoire of similar catalysts to other chemical evolution models. With minimal modifications, the model could be adjusted to study the possible chemical evolution of FeS or MoS cluster bearing proteins, e.g., ferredoxins, hydrogenases, and nitrogenases [42]. Utilizing NCs rather than bulk surfaces as a model for possible cluster precursors permits the investigation of size-dependent properties. The concept of hyperbranched scaffolds could also be applicable broadly to the models of chemical evolution. In these models, cofactors other than metal sulfides, i.e., small molecules and cations could be used. Furthermore, in lieu of hyperbranched polyimides and polyester, other polymers could be utilized, i.e., hyperbranched polyamidoamines [43] and polypeptides [44]. In addition to forming efficient

prebiotically plausible catalysts, the structure of cofactors scaffolded by globular polymers, superficially similar to contemporary enzymes, is intriguing in the context of chemical evolution as well. When considering enzyme-like prebiotic catalysts, the abundance of particular small-molecule cofactors, inorganic clusters, and cations are conceivable; however, functional high proteins and RNA molecules are unlikely to have been present at the early stages of chemical evolution. Several studies have tackled the prebiotic formation of peptide [45,46] and phosphodiester bonds [16,47]. These studies, however, so far, did not address the mechanisms controlling the primary structure of a biopolymer that is responsible for folding and function. The intrinsically globular hyperbranched polymers are a reasonable candidate for primitive protoenzymatic scaffolds.

In summary, we have presented a straightforward, plausibly prebiotic process of a spontaneous formation of stabilized polymer-supported nanoparticles. The structure of these complexes, a catalytic agent scaffolded by globular polymers, is superficially reminiscent of the enzymatic structure and therefore is a compelling model for the study of the chemical evolution of enzymes. An enzyme could be described as a catalytic agent augmented by a biopolymer scaffold. The hyperbranched polymer scaffold could have been the early primitive augmenting scaffold to be replaced with more sophisticated ones throughout chemical evolution. This primitive scaffold furthermore provides a means to study the aspects of small particle catalysis in prebiotic chemistry. Although herein, we have only explored the photocatalytic ZnS NC complex relevant to the "Zinc world" hypothesis of the origin of life, the model, however, can be easily extended to other protoenzymatic systems.

Supplementary Materials: The following are available online at www.mdpi.com/xxx/s1, Figure S1: MALDI mass spectrum of the $ZnCl_2$-bearing glycerol citrate polyester, Figure S2: Time-lapse measurement of photodegradation of eosin B ($5.0x10^{-5}$M, 30mL) under additional conditions, Figure S3: Visual progression of the eosin B degradation assay catalyzed by unsupported ZnS.

Author Contributions: Conceptualization, I.M.; methodology, I.M. and T.Z.J; formal analysis, I.M., M.C. and T.Z.J; investigation, I.M and M.C; resources, I.M and T.Z.J; writing—original draft preparation, I.M; writing—review and editing, I.M, M.C. and T.Z.J.; visualization, I.M.; funding acquisition, I.M. and T.Z.J. All authors have read and agreed to the published version of the manuscript.

Funding: This research was supported by the World Premier International Research Center Initiative (WPI), Ministry of Education, Culture, Sports, Science and Technology, Japan, as well as Grant-in-Aid for Scientific Research from the Japan Society for the Promotion of Science Kakenhi Kiban C Grant 17K01943 (to I.M.) and Wakate Grant 18K14354 (to T.Z.J.), as well as a Tokyo Institute of Technology Seed Grant "Tane" 1798 (to T.Z.J.).

Acknowledgments: We would like to thank Ryohei Kikuchi and Akira Genseki at the Tokyo Institute of Technology Ookayama Materials Analysis Division, Technical Department for assistance in TEM images.

Conflicts of Interest: The authors declare no conflict of interest.

References

1. Campbell, M. K.Farrell, S. O. *Biochemistry*; Cengage Learning, 2011.
2. Radzicka, A.; Wolfenden, R. A Proficient Enzyme. *Science* **1995**, *267 (5194)*, 90–93.
3. Richard, J. P.; Amyes, T. L.; Reyes, A. C. Orotidine 5'-Monophosphate Decarboxylase: Probing the Limits of the Possible for Enzyme Catalysis. *Acc. Chem. Res.* **2018**, *51 (4)*, 960–969.
4. Szöke, A.; Scott, W. G.; Hajdu, J. Catalysis, Evolution and Life. *FEBS Lett.* **2003**, *553 (1)*, 18–20.
5. Canepa, C. The Role of Catalysis on the Formation of an Active Proto-Enzyme in the Prebiotic Aqueous *Environment. Nat. Sc*i. **2013**, *05 (05)*, 549–555.
6. Kruger, K.; Grabowski, P. J.; Zaug, A. J.; Sands, J.; Gottschling, D. E.; Cech, T. R. Self-Splicing RNA: Autoexcision and Autocyclization of the Ribosomal RNA Intervening Sequence of Tetrahymena. *Cell* **1982**, *31 (1)*, 147–157.
7. Guerrier-Takada, C.; Gardiner, K.; Marsh, T.; Pace, N.; Altman, S. The RNA Moiety of Ribonuclease P Is the Catalytic Subunit of the Enzyme. *Cell* **1983**, *35 (3, Part 2)*, 849–857.

8. Cech, T. R. The RNA Worlds in Context. *Cold Spring Harb. Perspect. Biol. Cold Spring Harb. Perspect. Biol.* **2012**, *4(7)*, a006742.
9. Orgel, L. E. Some Consequences of the RNA World Hypothesis. *Orig. Life Evol. Biosph.* **2003**, *33 (2)*, 211–218.
10. Morowitz, H. J.; Srinivasan, V.; Smith, E. Ligand Field Theory and the Origin of Life as an Emergent Feature of the Periodic Table of Elements. *Biol. Bull.* **2010**, *219 (1)*, 1–6.
11. Shapiro, R. Small Molecule Interactions Were Central to the Origin of Life. *Q. Rev. Biol.* **2006**, *81 (2)*, 105–125.
12. Cleaves, H. J.; Scott, A. M.; Hill, F. C.; Leszczynski, J.; Sahai, N.; Hazen, R. Mineral–Organic Interfacial Processes: Potential Roles in the Origins of Life. *Chem. Soc. Rev.* **2012**, *41 (16)*, 5502–5525.
13. Russell, M. J.; Barge, L. M.; Bhartia, R.; Bocanegra, D.; Bracher, P. J.; Branscomb, E.; Kidd, R.; McGlynn, S.; Meier, D. H.; Nitschke, W.; Shibya T.; Vance S., White L.; Kanik I. Drive to Life on Wet and Icy Worlds. *Astrobiology* **2014**, *14 (4)*, 308–343
14. Bruice, T. C.; Benkovic, S. J. Chemical Basis for Enzyme Catalysis. *Biochemistry* **2000**, *39 (21)*, 6267–6274.
15. Hansma, H. G. Possible Origin of Life between Mica Sheets: Does Life Imitate Mica? *J. Biomol. Struct. Dyn.* **2013**, *31 (8)*, 888–895.
16. Ferris, J. P.; Hill, A. R.; Liu, R.; Orgel, L. E. Synthesis of Long Prebiotic Oligomers on Mineral Surfaces. *Nature* **1996**, *381 (6577)*, 59–61.
17. Kitadai, N.; Oonishi, H.; Umemoto, K.; Usui, T.; Fukushi, K.; Nakashima, S. Glycine Polymerization on Oxide Minerals. *Orig. Life Evol. Biosphere* **2017**, *47 (2)*, 123–143.
18. Breslow, R. Biomimetic Chemistry and Artificial Enzymes: Catalysis by Design. *Acc. Chem. Res.* **1995**, *28 (3)*, 146–153.
19. Kuah, E.; Toh, S.; Yee, J.; Ma, Q.; Gao, Z. Enzyme Mimics: Advances and Applications. Chem. – Eur. J. **2016**, *22 (25)*, 8404–8430.
20. Moshfegh, A. Z. Nanoparticle Catalysts. *J. Phys. Appl. Phys.* **2009**, *42 (23)*, 233001.
21. Liang, M.; Yan, X. Nanozymes: From New Concepts, Mechanisms, and Standards to Applications. *Acc. Chem. Res.* **2019**, *52 (8)*, 2190–2200.
22. Griffin, S.; Masood, M. I.; Nasim, M. J.; Sarfraz, M.; Ebokaiwe, A. P.; Schäfer, K.-H.; Keck, C. M.; Jacob, C. Natural Nanoparticles: A Particular Matter Inspired by Nature. *Antioxidants* **2017**, *7 (1)*, 3.
23. Hochella, M. F.; Lower, S. K.; Maurice, P. A.; Penn, R. L.; Sahai, N.; Sparks, D. L.; Twining, B. S. Nanominerals, Mineral Nanoparticles, and Earth Systems. *Science* **2008**, *319 (5870)*, 1631–1635.
24. Wächtershäuser, G. Groundworks for an Evolutionary Biochemistry: The Iron-Sulphur World. Prog. *Biophys. Mol. Biol.* **1992**, 58 (2), 85–201.
25. Mulkidjanian, A. Y. On the Origin of Life in the Zinc World: 1. Photosynthesizing, Porous Edifices Built of Hydrothermally Precipitated Zinc Sulfide as Cradles of Life on Earth. *Biol. Direct* **2009**, 4, 26.
26. Stroyuk, A. L.; Raevskaya, A. E.; Korzhak, A. V.; Kuchmii, S. Y. Zinc Sulfide Nanoparticles: Spectral Properties and Photocatalytic Activity in Metals Reduction Reactions. *J. Nanoparticle Res*. **2007**, *9 (6)*, 1027–1039.
27. Sarkar, S.; Guibal, E.; Quignard, F.; SenGupta, A. K. Polymer-Supported Metals and Metal Oxide Nanoparticles: Synthesis, Characterization, and Applications. *J. Nanoparticle Res.* **2012**, *14 (2)*, 715.
28. Donegá, C. de M. Synthesis and Properties of Colloidal Heteronanocrystals. *Chem. Soc. Rev.* **2011**, *40 (3)*, 1512–1546.
29. Campisi, S.; Schiavoni, M.; Chan-Thaw, C. E.; Villa, A. Untangling the Role of the Capping Agent in Nanocatalysis: Recent Advances and Perspectives. *Catalysts* **2016**, *6 (12)*, 185.
30. Kirkorian, K.; Ellis, A.; Twyman, L. J. Catalytic Hyperbranched Polymers as Enzyme Mimics; Exploiting the Principles of Encapsulation and Supramolecular Chemistry. *Chem. Soc. Rev.* **2012**, *41 (18)*, 6138–6159.
31. Liu, L.; Breslow, R. Dendrimeric Pyridoxamine Enzyme Mimics. *J. Am. Chem. Soc.* **2003**, *125 (40)*, 12110–12111.
32. Astruc, D.; Chardac, F. Dendritic Catalysts and Dendrimers in Catalysis. *Chem. Rev.* **2001**, *101 (9)*, 2991–3024.
33. Mamajanov, I.; Callahan, M. P.; Dworkin, J. P.; Cody, G. D. Prebiotic Alternatives to Proteins: Structure and Function of Hyperbranched Polyesters. *Orig. Life Evol. Biospheres* **2015**, *45(1-2)*, 123-137
34. Mamajanov, I. Wet-Dry Cycling Delays the Gelation of Hyperbranched Polyesters: Implications to the Origin of Life. *Life* **2019**, 9 (3).

35. Mamajanov I. Selective Synthesis of Hyperbranched Polyesters under Wet-Dry Cycling Conditions *ALife Conference Procedings*, **2018**, 580-581.
36. Mamajanov, I.; Cody, G. D. Protoenzymes: The Case of Hyperbranched Polyesters. *Philos. Trans. R. Soc. Math. Phys. Eng. Sci.* **2017**, *375(2109)*, 20160537.
37. Hassan, M. L.; Ali, A. F. Synthesis of Nanostructured Cadmium and Zinc Sulfides in Aqueous Solutions of Hyperbranched Polyethyleneimine. *Cryst. Growth* **2008**, *310*, 5252–5258.
38. Jia, J.; Wu, A.; Luan, S. Spectrometry Recognition of Polyethyleneimine towards Heavy Metal Ions. Colloids Surf. *Colloids Surf. Physicochem. Eng. Asp.* **2014**, *449*, 1–7.
39. Sang, L.-J.; Wu, Y.-Y.; Wang, H.-F. Polyethyleneimine/Manganese-Doped ZnS Nanocomposites: A Multifunctional Probe for Two-Color Imaging and Three-Dimensional Sensing. *ChemPlusChem* **2013**, *78* (5), 423–429.
40. Drexler, K. E. Molecular Imprinting: The Missing Piece in the Puzzle of Abiogenesis? arXiv:1807.07065 [q-bio.PE] **2018**.
41. Hu, J.-S.; Ren, L.-L.; Guo, Y.-G.; Liang, H.-P.; Cao, A.-M.; Wan, L.-J.; Bai, C.-L. Mass Production and High Photocatalytic Activity of ZnS Nanoporous Nanoparticles. *Angew. Chem.* **2005**, *117*, 1295–1299.
42. Stiefel, E. I.; George, G. N. 7 Ferredoxins , Hydrogenases , and Nitrogenases : Metal-Sulfide Proteins. *Bioorganic Chemistry* (Eds.: I. Bertini, H. B. Gray, S. J. Lippard, J. S. Valentine), University Science Books, Mill Valley, **1994**, pp. 365-453.
43. Pérignon, N.; Marty, J.-D.; Mingotaud, A.-F.; Dumont, M.; Rico-Lattes, I.; Mingotaud, C. Hyperbranched Polymers Analogous to PAMAM Dendrimers for the Formation and Stabilization of Gold Nanoparticles. *Macromolecules* **2007**, *40*, 3034–3041.
44. Peng, Q.; Zhu, J.; Yu, Y.; Hoffman, L.; Yang, X. Hyperbranched Lysine−Arginine Copolymer for Gene Delivery. *J. Biomater. Sci. Polym. Ed.* **2015**, *26*, 1–35.
45. Forsythe, J. G.; Yu, S.-S.; Mamajanov, I.; Grover, M. A.; Krishnamurthy, R.; Fernández, F. M.; Hud, N. V. Ester-Mediated Amide Bond Formation Driven by Wet–Dry Cycles: A Possible Path to Polypeptides on the Prebiotic Earth. *Angew. Chem. Int. Ed.* **2015**, *54*, 9871–9875
46. Rodriguez-Garcia, M.; Surman, A. J.; Cooper, G. J. T.; Suárez-Marina, I.; Hosni, Z.; Lee, M. P.; Cronin, L. Formation of Oligopeptides in High Yield under Simple Programmable Conditions. *Nat. Commun.* **2015**, *6*, 8385.
47. Costanzo, G.; Pino, S.; Ciciriello, F.; Mauro, E. D. Generation of Long RNA Chains in Water. *J. Biol. Chem.* **2009**, *284* (48), 33206–33216.

Supplementary Materials

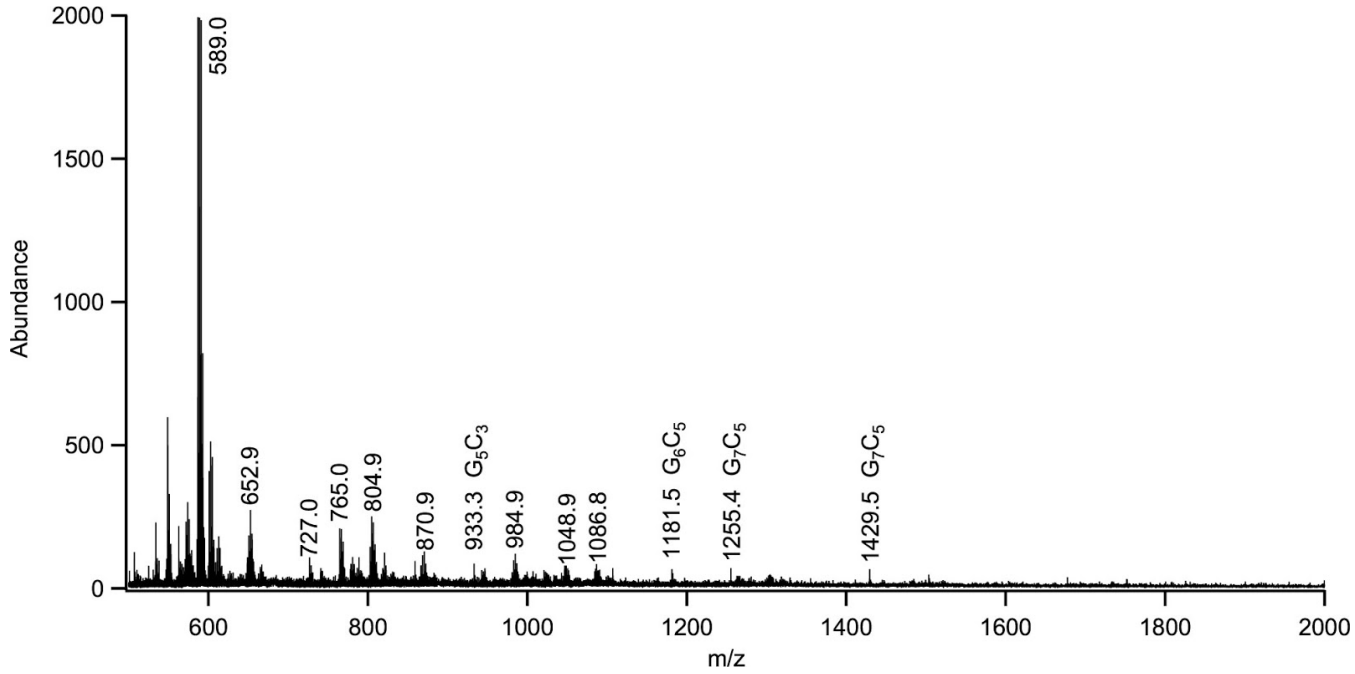

Figure S1. MALDI mass spectrum of the $ZnCl_2$-bearing glycerol citrate polyester. The mass spec is indicative of a heterogeneous mixture of polymeric species. The assigned peaks indicate the masses consistent with molecular formulae of x glycerol (G) units and y citrate units (C). The assignments were possible in the case of sodiated signals; zinc complexes were difficult to assign unequivocally due to the complexity of the zinc isotopic pattern.

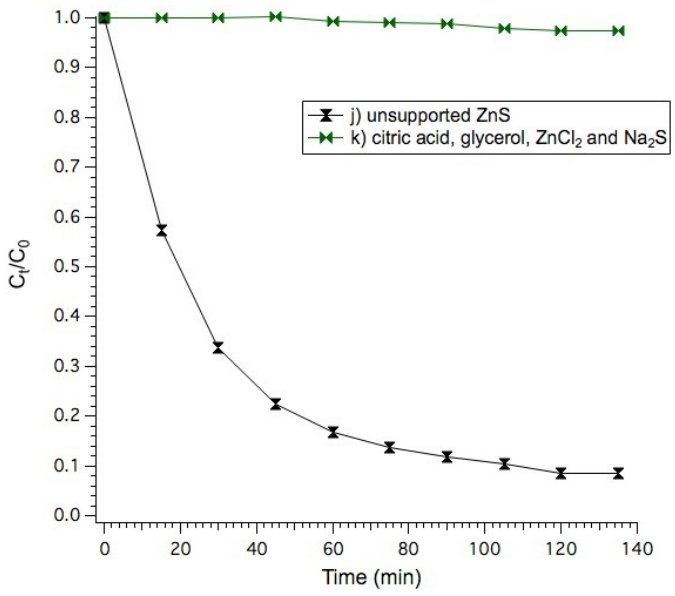

Figure S2. Time-lapse measurement of photodegradation of eosin B ($5.0x10^{-5}$M, 30mL) under additional conditions: j) with unsupported ZnS particles, under UV, k) with *unreacted* citric acid, glycerol, $ZnCl_2$, Na_2S,

under UV.

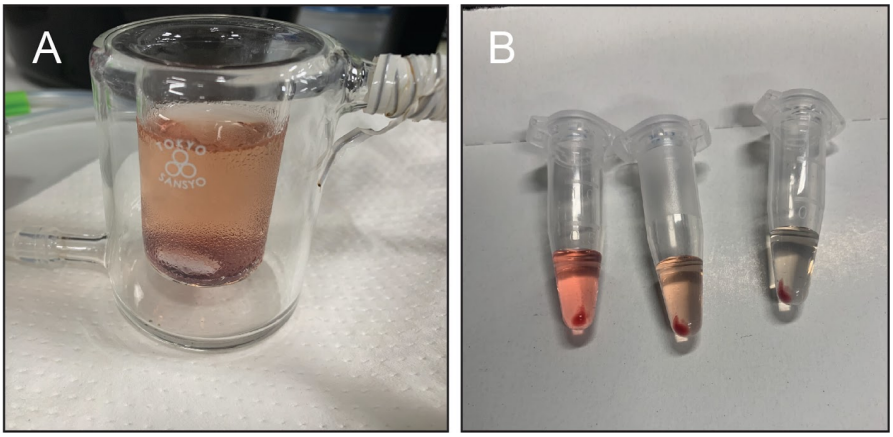

Figure S3. Visual progression of the eosin B degradation assay catalyzed by unsupported ZnS. A) Photograph of the reaction vessel showing colored precipitate at the end of the reaction. B) Photograph of the centrifuged aliquots taken over the course of the measurement (left to right indicates increasing time) featuring the colored precipitate.